Liquid Crystals

Publication details, including instructions for authors and subscription information:
http://www.informaworld.com/smpp/title~content=t713926090

New antiferroelectric liquid crystalline materials containing a keto group and two lactate groups

Věra Hamplová[a]; Alexej Bubnov Corresponding author[a]; Miroslav Kašpar[a]; Vladimíra Novotná[a]; Yveta Lhotáková[a]; Milada Glogarová[a]
[a] Institute of Physics, Academy of Sciences of the Czech Republic, 182 21 Prague, Czech Republic

To cite this Article Hamplová, Věra , Bubnov Corresponding author, Alexej , Kašpar, Miroslav , Novotná, Vladimíra , Lhotáková, Yveta and Glogarová, Milada(2003) 'New antiferroelectric liquid crystalline materials containing a keto group and two lactate groups', Liquid Crystals, 30: 12, 1463 — 1469

To link to this Article: DOI: 10.1080/02678290310001622506

URL: http://dx.doi.org/10.1080/02678290310001622506

LIQUID CRYSTALS, VOL. 30, NO. 12, DECEMBER 2003, 1463–1469

Taylor & Francis
Taylor & Francis Group

New antiferroelectric liquid crystalline materials containing a keto group and two lactate groups

VĚRA HAMPLOVÁ, ALEXEJ BUBNOV*, MIROSLAV KAŠPAR,
VLADIMÍRA NOVOTNÁ, YVETA LHOTÁKOVÁ and
MILADA GLOGAROVÁ

Institute of Physics, Academy of Sciences of the Czech Republic, Na Slovance 2,
182 21 Prague, Czech Republic

(*Received 14 March 2003; in final form 16 June 2003; accepted 21 July 2003*)

New chiral liquid crystalline materials containing a keto group and two lactate units attached to the mesogenic core have been synthesized and studied. All the new compounds show the paraelectric SmA, ferroelectric SmC* and antiferroelectric SmC*$_A$ phases each over rather broad temperature ranges. The properties of the phases were characterized by DSC, electro-optical and dielectric studies. The spontaneous polarization, tilt angle, helical pitch, and switching times were determined for the polar phases.

1. Introduction

Since the discovery of the antiferroelectric SmC*$_A$ phase for MHPOBC [1], it has been observed in many substances. Antiferroelectric liquid crystals are still of great interest not only due to their application potential but also on a fundamental level because of the anticlinic structure of the phase. The relationships between their molecular structure and physical properties are not clearly understood. In designing new liquid crystal molecules, we must remember that their mesogenic behaviour is influenced not only by the structure of the rigid molecular core but also by the chiral part of the molecule. Using the lactate unit as the basis of the chiral segment has yielded many materials having a rather broad ferroelectric phases [2–6]. Materials containing two lactate units have been described in just a few papers [7–9] although some of these showed the antiferroelectric phase.

Recently, two new series of liquid crystalline materials containing two lactate units in the chiral part of the molecule were synthesized and studied [7]. These compounds show the paraelectric SmA phase, the ferroelectric SmC* phase and a hexatic phase. Some of these, specifically those having three chiral centres, also exhibit the antiferroelectric SmC*$_A$ phase.

More recently, two series of new ferroelectric liquid crystalline materials containing a keto group in the core and one lactate unit have been described [10]. In these materials, the transverse dipole moment near the chiral centre becomes dominant due to the weakening of the longitudinal molecular dipole moment. These compounds show a wide ferroelectric SmC* phase with rather high values of spontaneous polarization down to room temperatures [10]. In the present work, we attempted to combine the promising chiral segment containing two lactate units with a keto group in the core with the aim of obtaining a broad antiferroelectric phase with high values of spontaneous polarization, such a material could meet application demands. The general formula of the materials studied, which are denoted as KLL*m*/*n*, is:

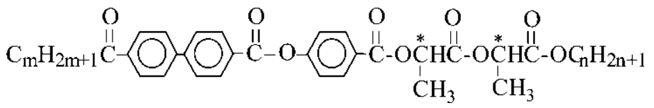

2. Synthesis

The general procedure for the preparation of the KLL*m*/*n* homologues is shown in the scheme.

The synthesis of the keto acids **1** has been described recently [10]. The synthesis of compounds **2** and **3** was described in detail in [7]. All chiral centres have (*S*) configuration. The final KLL*m*/*n* products were prepared by the reaction of 10 mmol of phenol **3** and 10 mmol of mesogenic acid **1** in 100 ml of dichloromethane after the addition of 15 mmol of *N*,*N*′-dicyclohexylcarbodiimide. The mixture was stirred for 12 h at room temperature. The crude product was chromatographed on silica gel (Kieselgel 60, Merck)

---

*Author for correspondence; e-mail: bubnov@fzu.cz

Liquid Crystals ISSN 0267-8292 print/ISSN 1366-5855 online
http://www.tandf.co.uk/journals
DOI: 10.1080/02678290310001622506

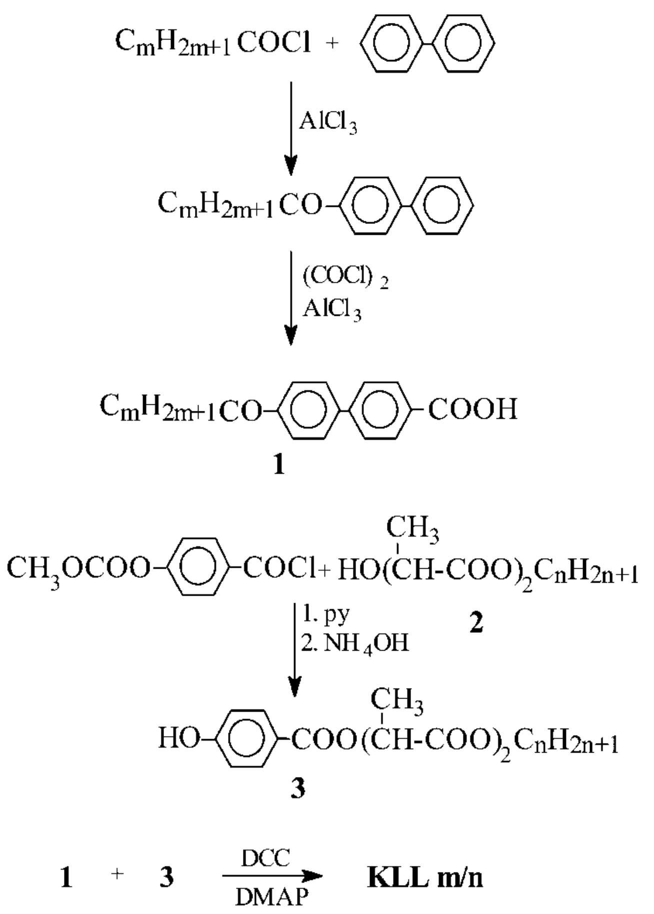

Scheme.

using a mixture of dichloromethane and acetone (99.5/0.5) as eluent. After crystallization from methanol, the structure of all prepared products was checked by ^{1}H NMR, and purity was determined by high performance liquid chromatography. The chemical purity of all synthesized compounds was between 99.5% and 99.9%.

^{1}H NMR (200 MHz, $CDCl_3$) for **2** ($n=6$) : 5.15 q (1H, C*H); 4.35 q (1H, C*HOH); 4.10 m (2H, CH_2 OCO); 1.65 quint. (2H, $\underline{CH_2}$ CH_2 O); 1.20–1.35 m (6H, CH_2); 1.50 d (3H, CH_3 C*); 1.45 d (3H, $\underline{CH_3}$ C*HOH); 0.88 t (3H, CH_3).

^{1}H NMR (200 MHz, $CDCl_3$) for **3** ($n=6$): 7.90 d (2H, ArH); 6.80 d (2H, ArH *ortho* to OH); 5.30 q (1H, ArCOO$\underline{\text{C*H}}$); 5.15 q (1H, $\underline{\text{C*H}}$COOR′); 4.10 m (2H, $COOCH_2$); 1.65 d (3H, ArCOOC*H$\underline{CH_3}$); 1.50 d (3H, $\underline{CH_3}$ C*H); 1.20–1.70 m (8H, CH_2); 0.90 t (3H, CH_3).

^{1}H NMR (200 MHz, $CDCl_3$) for KLL6/8: 8.30 d (2H,HAr *ortho* to –COOAr); 8.20 d (2H, HAr *ortho* to COOC*); 8.08 d (2H, HAr *ortho* to –CO–); 7.75 m (4H, HAr *ortho* to – Ar); 7.35 d (2H, HAr *ortho* to –OCO); 5.40 q (1H, ArCOO$\underline{\text{C*H}}$); 5.20 q (1H, C*H COOR); 4.15 t (2H, $COOCH_2$); 3.00 t (2H, CH_2 COAr); 1.75 d (3H, ArCOOC*H$\underline{CH_3}$); 1.55 d (3H, $\underline{CH_3}$ C*H); 1.20–1.70 m (20H, CH_2); 0.90 m (6H, CH_3).

3. Characterization

All the materials synthesized were studied by DSC (Pyris Diamond Perkin-Elmer 7) using cooling and heating runs at a rate of 5 K min^{-1}. The samples of 3–8 mg were placed in a nitrogen atmosphere and hermetically sealed in aluminium pans.

Texture and physical studies were carried out using glass cells filled by means of capillary action with ITO transparent electrodes (5×5 mm^2) and polyimide layers unidirectionally rubbed, which ensured planar aligned (quasi-bookshelf) geometry. The temperature stability was better than 0.1 K. The sample thickness was defined by mylar sheets as 25 µm. Thicker cells (up to 100 µm) were used only for helical pitch measurements. The alignment was improved using an electric field (10–20 Hz, 40 kV cm^{-1}) applied for about 5–20 min.

Values of spontaneous polarization ($\mathbf{P}_s$) were evaluated from the $\mathbf{P}(\mathbf{E})$ hysteresis loop detected during $\mathbf{P}_s$ switching in an a.c. electric field $\mathbf{E}$ of frequency 60 Hz. The spontaneous tilt angle (θ_s) was determined optically from the difference between extinction positions detected at crossed polarizers under opposite d.c. electric fields of ± 40 kV cm^{-1}. A memory oscilloscope, leCroy 9304, provided the switching current versus time. The position of the switching current peaks on the time axis represents the switching time (τ).

Values of the helical pitch length (p) were obtained from the diffraction of He-Ne laser light (632 nm) by the helix unwinding lines (disclination lines), which exist in planar samples due to the strong polar anchoring at the surfaces. This method can be used only for the measurement of the helical pitch of a limited length. For pitches shorter than 0.7 µm the diffraction ring is diffuse or completely disappears. If the equilibrium pitch is longer than a few µm the helix may become non-regular or can be completely unwound by surface anchoring.

Free-standing films (i.e. without a glass support) were used for the optical rotatory power (ρ) measurements. In this method the rotation of the plane of the polarized light is measured, which yields information of relative changes of the molecular spiralling along the helical axis with temperature; however, the absolute value of the pitch length cannot be evaluated. In free-standing films the helix pitch length within the visible range wavelength can be evaluated from the selective reflection of a definite light colour.

For all compounds studied, the real and imaginary parts of complex permittivity were measured on cooling as a function of frequency using a Schlumberger 1260 impedance analyser in the frequency range 1 Hz–1 MHz, keeping the temperature of the sample stable to within

±0.1 K during frequency sweeps. Planar aligned samples were used for these studies. The data obtained were analysed over the whole temperature range of the SmA, SmC* and SmC*$_A$ phases using the Cole–Cole formula for the frequency-dependent complex permittivity $\varepsilon^*(f)=\varepsilon'-\mathrm{i}\varepsilon''$:

$$\varepsilon^* - \varepsilon_\infty = \frac{\Delta\varepsilon}{1+(\mathrm{i}f/f_\mathrm{r})^{(1-\alpha)}} - \mathrm{i}\frac{\sigma}{2\pi\varepsilon_0 f^n} + Af^m$$

where f_r is the relaxation frequency, $\Delta\varepsilon$ is the dielectric strength, α is the distribution parameter of the mode, ε_0 is the permittivity of vacuum, ε_∞ is the high frequency permittivity and n, m, A are fitting parameters. The second and third terms on the right hand side of the equation are used to eliminate a low frequency contribution to ε'' from the d.c. conductivity σ and the high frequency contribution from the ITO electrodes, respectively.

4. Results

4.1. *Mesomorphic properties*

For all the substances studied, phase sequences and transition temperatures were determined from characteristic textures and their changes observed under a polarizing microscope (Nikon Eclipse E600POL) on cooling from the isotropic phase and verified by DSC measurements (see the table).

All the compounds synthesized show the paraelectric SmA phase, the ferroelectric SmC* phase and the antiferroelectric SmC*$_A$ phase over rather wide temperature ranges. Phase diagrams for the KLL 6/*n* and KLL 8/*n* homologues are shown in figure 1 (*a*) and (*b*), respectively. The chain length has no significant effect on the temperature range of the phases. However, KLL 8/4 shows a wider temperature range for the antiferroelectric phase down to 32°C. For all the compounds studied, the SmC*$_A$ phase is entirely (KLL 6/6) or partly monotropic as the melting points are some 20–30 K higher than the crystallization temperatures (see the table).

4.2. *Spontaneous quantities*

Values of the spontaneous tilt angle (θ_s) and spontaneous polarization ($\mathbf{P}_\mathrm{s}$) increase continuously from zero as the temperature decreases from the

Table. Melting points (°C), phase transition temperatures (°C) and transition enthalpies [ΔH (J g^{-1})] from DSC measurements obtained on cooling (5 K min^{-1}) for the KLL *m*/*n* compounds (● indicates the existence of a phase).

Compound	m.p.	Cr		SmC$_A$*		SmC*		SmA		I
KLL 6/4	89 [21.7]	●	53 [−13.1]	●	96 [−0.1]	●	110 [−0.9]	●	145 [−3.8]	●
KLL 6/5	78 [29.4]	●	52 [−24.2]	●	95 [−0.1]	●	114 [−0.1]	●	139 [−6.2]	●
KLL 6/6	90 [51.3]	●	53 [−23.7]	●	90 [−0.2]	●	108 [−0.5]	●	133 [−5.7]	●
KLL 8/4	68 [19.4]	●	32 [−9.1]	●	79 [−0.1]	●	108 [−0.1]	●	135 [−2.7]	●
KLL 8/5	77 [29.2]	●	56 [−23.7]	●	78 [−0.02]	●	111 [−0.3]	●	128 [−4.9]	●
KLL 8/6	70 [23.1]	●	52 [−21.1]	●	76 [−0.1]	●	104 [−0.5]	●	124 [−4.0]	●

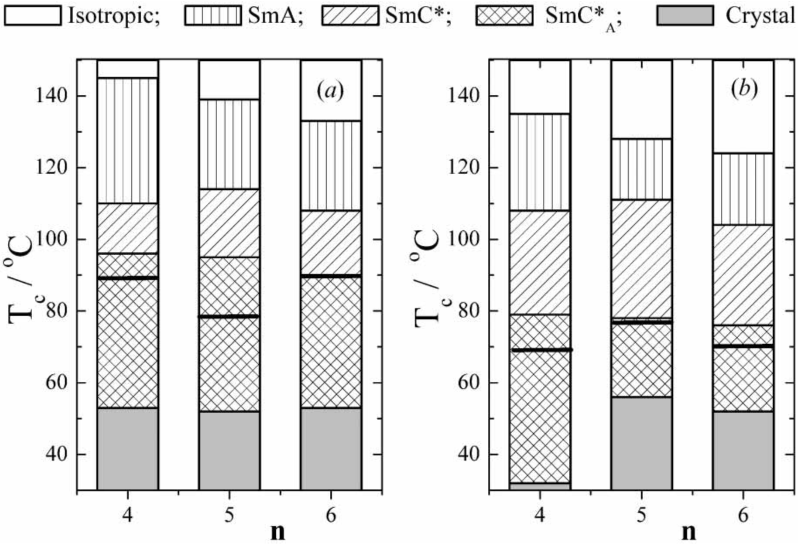

Figure 1. Phase diagrams for (*a*) KLL 6/*n* and (*b*) KLL 8/*n* homologues determined on cooling. Thick solid lines indicate the melting points.

SmA–SmC* phase transition. This behaviour is typical for a second order phase transition. The values of spontaneous polarization exhibit no saturation and reach 190 nC cm^{-2} at the low limit of the SmC*$_A$ phase (see figure 2). For all compounds, θ_s reaches about 31–35° at saturation (see figure 3). For these compounds a linear $\mathbf{P}_s$ (θ_s) relationship does not hold. Similar behaviour has been observed also for materials based on lactic acid having differing chemical structures [10–14]. In the case of lactic acid derivatives, the competition between different conformers must be considered. It was shown [15] that the continuous increase of the spontaneous polarization may be explained by the increase in concentration of conformers having the higher transverse dipole moment.

At the SmC*→SmC*$_A$ phase transition, no anomalies in the $\mathbf{P}_s(T)$ and $\theta_s(T)$ plots are seen (see figure 2 and 3, respectively). For compound KLL 8/4, the measurement of $\mathbf{P}_s$ and θ_s could not be made down to the low limit of the SmC*$_A$ phase as the required field increased strongly below 50°C.

For selected KLL compounds, the temperature dependence of the helical pitch length (p) in the SmC* phase is shown in figure 4. For compound KLL 8/4, p is nearly temperature independent with just a slight increase on cooling over the whole temperature range of the SmC* phase. For the other materials close to or below the transition to the ferroelectric SmC* phase, the helical pitch reached 4 μm and could not be measured at lower temperatures as the spacing between helix unwinding lines became rather high and irregular, completely disappearing on approaching the SmC*$_A$ phase. This indicates the unwinding of the helix in the SmC* phase. The continuous increase of the helix pitch up to the unwinding was confirmed by optical rotatory power measurements on free-standing films; see figures 5 (*a*) and 5 (*b*) for KLL 6/5 and KLL 8/5, respectively.

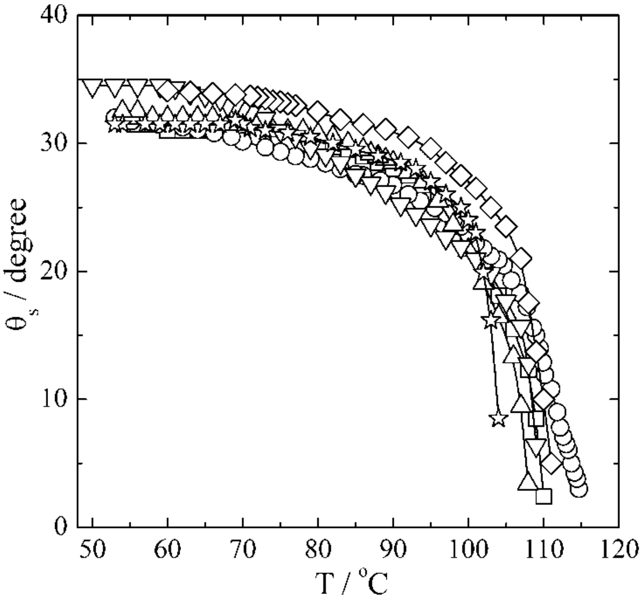

Figure 3. Temperature dependence of the spontaneous tilt angle $\theta_s(T)$ for KLL m/n homologues; □ = KLL 6/4; ○ = KLL 6/5; △ = KLL 6/6; ▽ = KLL 8/4; ◇ = KLL 8/5 and ☆ = KLL 8/6.

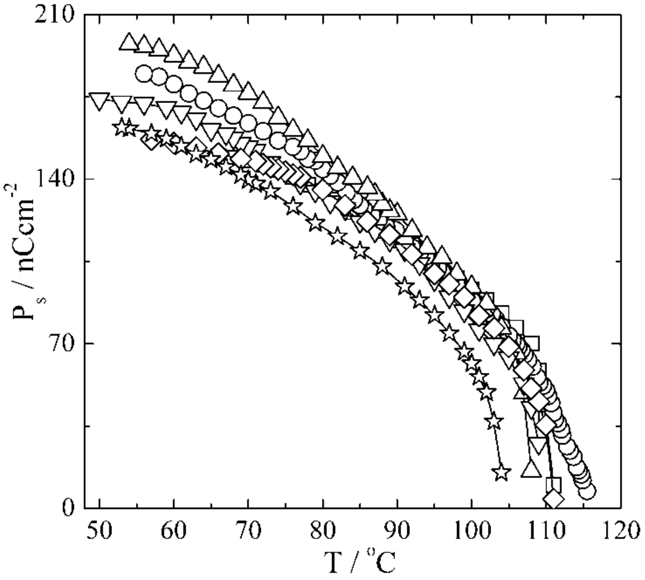

Figure 2. Temperature dependence of the spontaneous polarization $\mathbf{P}_s(T)$ for KLL m/n homologues; □ = KLL 6/4; ○ = KLL 6/5; △ = KLL 6/6; ▽ = KLL 8/4; ◇ = KLL 8/5 and ☆ = KLL 8/6.

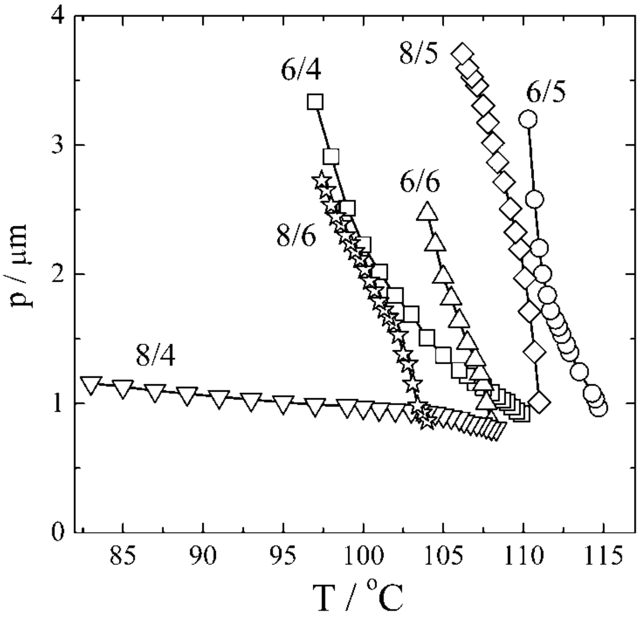

Figure 4. Temperature dependence of the helical pitch length $p(T)$ for KLL m/n homologues.

In the antiferroelectric SmC*$_A$ phase, the helix unwinding lines were not seen. The sample became colourful and the colours changing with varying temperature. The colours are due to selective reflection of the light by the helix unwinding lines, the spacing of which is comparable with the wavelength of the reflected light.

4.3. *Switching properties*

In the polar phases, switching properties were studied under a square wave electric field by measuring the current density as a function of time. In figure 6 the switching time τ, evaluated as a time delay between the pulse edge and the current peak, is shown as a function of temperature for two compounds revealing typical behaviour. The values of the switching time increase from tens of μs below T_c (SmA→SmC* phase transition) to values of about one ms when approaching crystallization at ~50°C on cooling. No anomalies at the SmC*→SmC*$_A$ phase transition were detected (see figure 6).

4.4. *Dielectric properties*

Figure 7 shows a typical frequency dependence of the imaginary part of permittivity for 25 μm thick cells measured in the temperature interval 120–50°C on cooling from the isotropic phase. Frequency dispersion data show the soft mode in the paraelectric SmA phase, the Goldstone mode in ferroelectric SmC* phase and a high frequency mode in the antiferroelectric SmC*$_A$ phase. The fitting of the data yields the relaxation frequency and dielectric strength, which are shown in figures 8 (*a*, *b*) and 9 (*a*, *b*), respectively. In the *paraelectric* SmA phase, the frequency of the soft mode

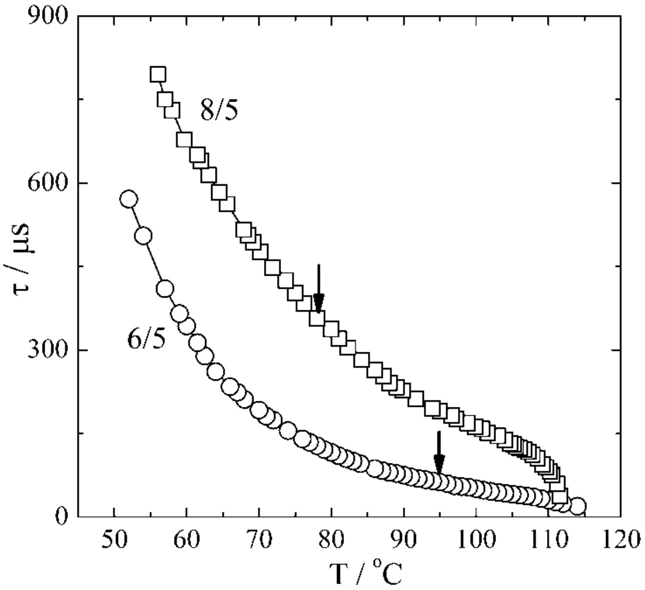

Figure 6. Temperature dependence of the switching time $\tau(T)$ for KLL 6/5 and KLL 8/5 over the whole temperature range of the ferroelectric and antiferroelectric phases. Arrows indicate the SmC*→SmC*$_A$ phase transition.

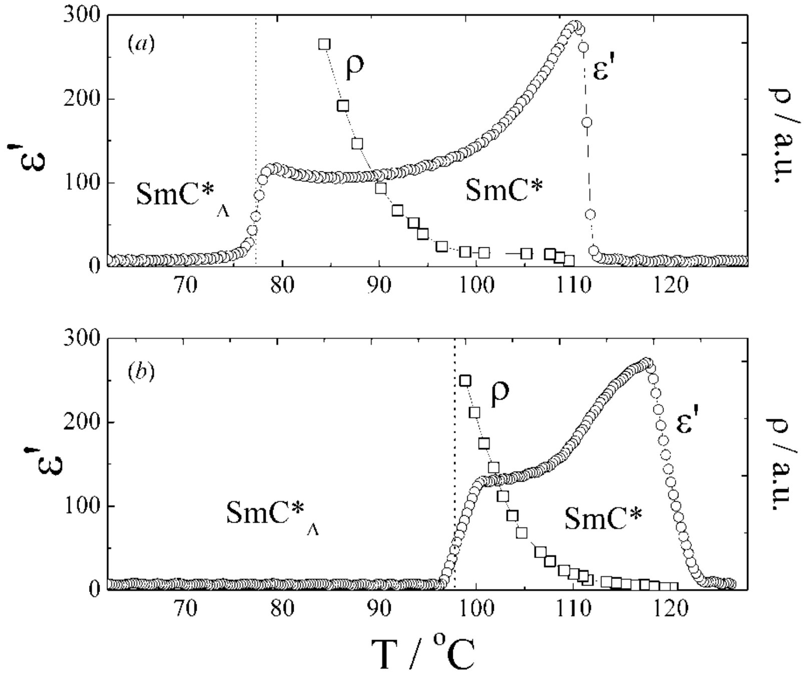

Figure 5. Temperature dependence of the optical rotatory power ρ and the real part of dielectric constant ε' measured at 100 Hz for compounds (*a*) KLL 6/5 and (*b*) KLL 8/5.

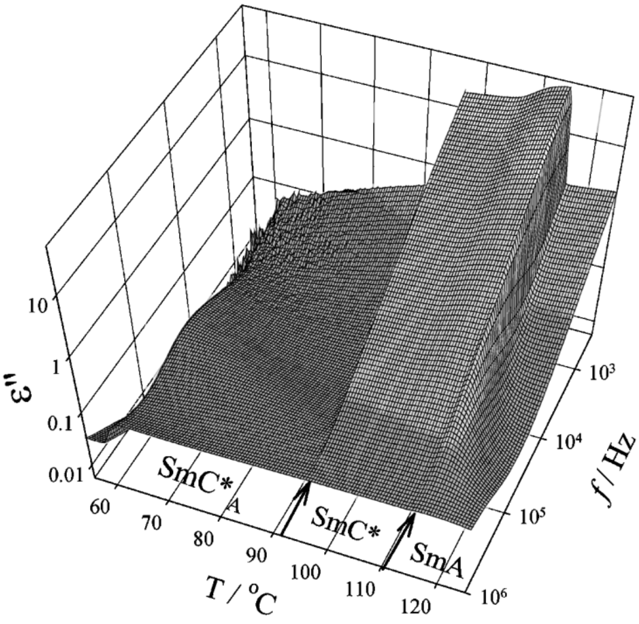

Figure 7. 3D plot of the imaginary part of permittivity for KLL 6/5 measured on cooling. Arrows indicate the phase transition temperatures.

decreases, and dielectric strength steeply increases, when approaching the transition temperature to the ferroelectric SmC* phase. In the *ferroelectric* SmC* phase, the relaxation frequency is very low and the dielectric strength is high, which is the typical feature of the Goldstone mode. In the *antiferroelectric* SmC*$_A$ phase, the high frequency mode was detected for all the compounds studied. This mode may be attributed to the anti-phase mode, in which the azimuthal director fluctuations deform the anticlinic ordering [16, 17].

5. Discussion and conclusions

All these new KLL *m*/*n* compounds containing two lactate units in the chiral chain and a keto group in the core show the *paraelectric* SmA phase, the *ferroelectric* SmC* phase and the *antiferroelectric* SmC*$_A$ phase, each over a rather broad temperature range. The ferroelectric and antiferroelectric smectic phases occur even for compounds with very short alkyl chains (down to $n=4$), which is rather unusual. KLL 8/4 shows a wider temperature range for the antiferroelectric phase than the other homologues.

If we compare the mesomorphic properties of compounds having the same core, but differing in the number of lactate groups in the chiral part and by the presence of the keto group between the non-chiral chain and the molecular core, we see that the antiferroelectric phase occurs in materials with two lactate groups whether [8, this paper] or not [7] they contain a keto group. On the other hand, homologues with one or three lactate groups exhibit no antiferroelectric phase, regardless of the presence of the keto group [2, 8, 10, 13]. One may conclude that in this type of compound the number of lactate groups is decisive for the occurrence of the antiferroelectric phase, while the keto group plays no role. Nevertheless, the keto group increases the temperature range and the values of spontaneous polarization of the polar phases (*cf.* [8, 10, this paper] and [2, 13]).

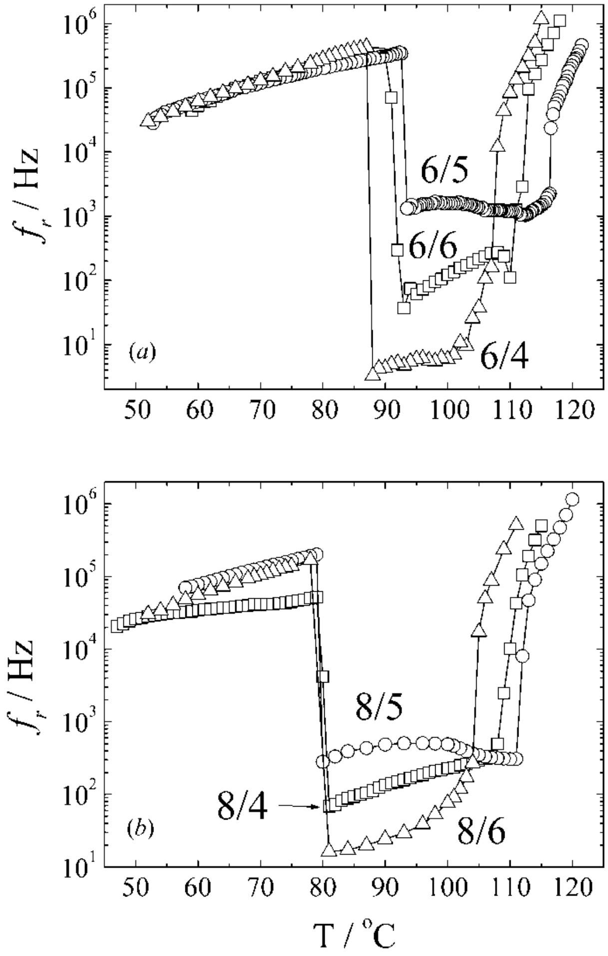

Figure 8. Temperature dependence of relaxation frequency $f_r(T)$ for (*a*) KLL 6/*n* and (*b*) KLL 8/*n* homologues over the whole temperature range of the paraelectric, ferroelectric and antiferroelectric phases. The abrupt changes correspond to phase transitions.

At the SmC*→SmC*$_A$ phase transition, no anomalies in the $\mathbf{P}_s(T)$ and $\theta_s(T)$ dependences were detected.

On cooling, the helical pitch length steeply increases within the SmC* phase up to the unwinding of the helical structure near to or below the SmA→SmC* phase transition. In the SmC*$_A$ phase, *p* becomes comparable to the wavelength of visible light.

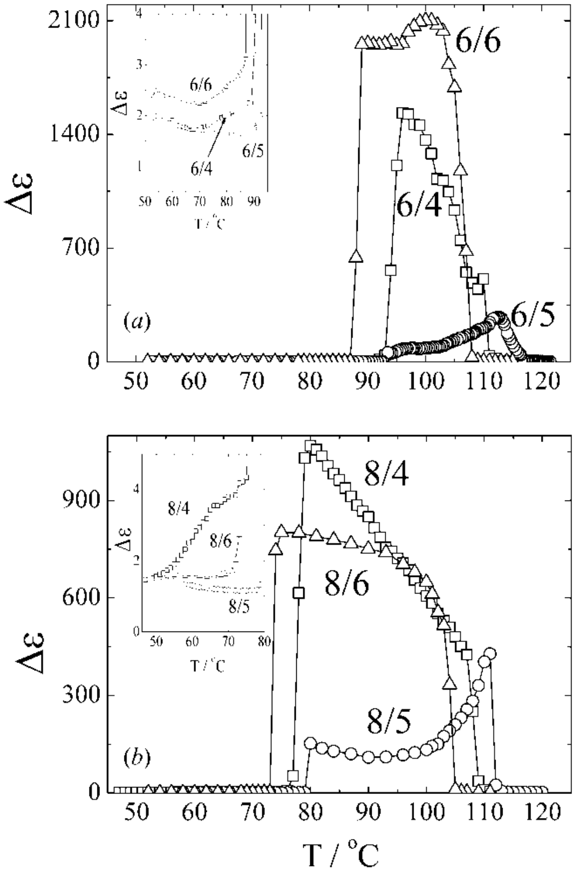

Figure 9. Temperature dependence of dielectric strength Δε (*T*) for (*a*) KLL 6/*n* and (*b*) KLL 8/*n* homologues over the whole temperature range of the paraelectric, ferroelectric and antiferroelectric phases. The abrupt changes correspond to phase transitions. In the inset, Δε (*T*) in the antiferroelectric phase is shown on an enlarged scale.

From the dielectric spectroscopy data, the dielectric strength of the Goldstone mode is remarkably smaller for KLL *m*/5 homologues than for KLL *m*/6 homologues. The dielectric strength of the Goldstone mode can be expressed by $\Delta\varepsilon_G \approx (1/8\pi^2 K)(p\ \mathbf{P}_s/\theta_s)^2$, where K is an elastic constant [18, 19]. As no remarkable difference in polarization, tilt angle or helical pitch were observed for all the homologues studied, only the relatively high elastic constant K (with respect to the other studied homologues), could explain the low values of the dielectric strength for KLL *m*/5 homologues.

In the *antiferroelectric* SmC*$_A$ phase, the high frequency anti-phase mode was detected for all the materials studied. The relaxation frequency of this mode decreases from some hundreds to several tens of kHz. This decrease can be explained by a gradual increase in viscosity while approaching low temperatures, which is also responsible for the increase of the switching time at lower temperatures.

This work was supported by Grants No. 202/03/P011, No. 202/02/0840 from the Grant Agency of the Czech Republic, European Project COST D014 WG00015 and Research Project AVOZ1-010-914.

References

[1] Chandani, A. D. L., Gorecka, E., Ouchi, Y., Takezoe, H., and Fukuda, A., 1989, *Jpn. J. appl. Phys.*, **28,** L1265.
[2] Tsai, W. L., Lu, T. C., Liu, H. W., Tsai, M. Y., and Fu, C. M., 2000, *Liq. Cryst.*, **27,** 1389.
[3] Taniguchi, H., Ozaki, M., Yoshino, K., Satoh, K., and Yamasaki, N., 1988, *Ferroelectrics*, **77,** 137.
[4] Tsai, W.-L., Yen, S.-W., Hsie, M.-J., Lee, H.-C., and Fu, C.-M., 2002, *Liq. Cryst.*, **29,** 251.
[5] Matsushima, J., Takanishi, Y., Ishikawa, K., Takezoe, H., Fukuda, A., Park, C. S., Jang, W.-G., Kim, K.-H., Maclennan, J.-E., Glaser, M. A., Clark, N. A., and Takanishi, K., 2002, *Liq. Cryst.*, **29,** 27.
[6] Bubnov, A., Hamplová, V., Kašpar, M., Glogarová, M., and Vaněk, P., 2000, *Ferroelectrics*, **243,** 27.
[7] Kašpar, M., Hamplová, V., Novotná, V., Glogarová, M., Pociecha, D., and Vaněk, P., 2001, *Liq. Cryst.*, **28,** 1203.
[8] Hamplová, V., Bubnov, A., Kašpar, M., Novotná, V., Pociecha, D., and Glogarová, M., 2003, *Liq. Cryst.*, **30,** 627.
[9] Mery, S., Lottzsch, D., Heppke, G., and Shashidhar, R., 1997, *Liq. Cryst.*, **23,** 629.
[10] Hamplová, V., Bubnov, A., Kašpar, M., Novotná, V., and Glogarová, M., 2003, *Liq. Cryst.*, **30,** 493.
[11] Novotná, V., Kašpar, M., Hamplová, V., and Glogarová, M., 2002, *Liq. Cryst.*, **29,** 1435.
[12] Kašpar, M., Hamplová, V., Pakhomov, S. A., Bubnov, A., Guittard, F., Sverenyák, H., Stibor, I., Vaněk, P., and Glogarová, M., 1998, *Liq. Cryst.*, **24,** 599.
[13] Wu, S. L., and Lin, C. Y., 2002, *Liq. Cryst.*, **29,** 1575.
[14] Wu, S. L., and Lin, C. Y., 2003, *Liq. Cryst.*, **30,** 471.
[15] Gorecka, E., Glogarová, M., Sverenyák, H., Kašpar, M., Hamplová, V., and Pakhomov, S. A. *Ferroelectrics*, **179**, 81.
[16] Gisse, P., Pavel, J., Nguyen, H. T., and Lorman, V. L., 1993, *Ferroelectrics*, **147,** 27.
[17] Novotná, V., Glogarová, M., Hamplová, V., and Kašpar, M., 2001, *J. chem. Phys.*, **115,** 9036.
[18] Blinc, R., and Žekš, B., 1978, *Phys. Rev. A*, **18,** 740.
[19] Carlsson, T., Žekš, B., Filipič, C., Levstik, A., and Blinc, R., 1988, *Mol. Cryst. liq. Cryst.*, **163,** 11.